

Observation of $Y(3S) \rightarrow \tau^+ \tau^-$ and Tests of Lepton Universality in Y Decays

D. Besson,¹ T. K. Pedlar,² D. Cronin-Hennessy,³ K. Y. Gao,³ D. T. Gong,³ J. Hietala,³ Y. Kubota,³ T. Klein,³ B. W. Lang,³ R. Poling,³ A. W. Scott,³ A. Smith,³ P. Zweber,³ S. Dobbs,⁴ Z. Metreveli,⁴ K. K. Seth,⁴ A. Tomaradze,⁴ J. Ernst,⁵ H. Severini,⁶ S. A. Dytman,⁷ W. Love,⁷ V. Savinov,⁷ O. Aquines,⁸ Z. Li,⁸ A. Lopez,⁸ S. Mehrabyan,⁸ H. Mendez,⁸ J. Ramirez,⁸ G. S. Huang,⁹ D. H. Miller,⁹ V. Pavlunin,⁹ B. Sanghi,⁹ I. P. J. Shipsey,⁹ B. Xin,⁹ G. S. Adams,¹⁰ M. Anderson,¹⁰ J. P. Cummings,¹⁰ I. Danko,¹⁰ J. Napolitano,¹⁰ Q. He,¹¹ J. Insler,¹¹ H. Muramatsu,¹¹ C. S. Park,¹¹ E. H. Thorndike,¹¹ F. Yang,¹¹ T. E. Coan,¹² Y. S. Gao,¹² F. Liu,¹² M. Artuso,¹³ S. Blusk,¹³ J. Butt,¹³ N. Horwitz,¹³ J. Li,¹³ N. Mena,¹³ R. Mountain,¹³ S. Nisar,¹³ K. Randrianarivony,¹³ R. Redjimi,¹³ R. Sia,¹³ T. Skwarnicki,¹³ S. Stone,¹³ J. C. Wang,¹³ K. Zhang,¹³ S. E. Csorna,¹⁴ G. Bonvicini,¹⁵ D. Cinabro,¹⁵ M. Dubrovin,¹⁵ A. Lincoln,¹⁵ D. M. Asner,¹⁶ K. W. Edwards,¹⁶ R. A. Briere,¹⁷ I. Brock,^{17,*} J. Chen,¹⁷ T. Ferguson,¹⁷ G. Tatishvili,¹⁷ H. Vogel,¹⁷ M. E. Watkins,¹⁷ J. L. Rosner,¹⁸ N. E. Adam,¹⁹ J. P. Alexander,¹⁹ K. Berkelman,¹⁹ D. G. Cassel,¹⁹ J. E. Duboscq,¹⁹ K. M. Ecklund,¹⁹ R. Ehrlich,¹⁹ L. Fields,¹⁹ R. S. Galik,¹⁹ L. Gibbons,¹⁹ R. Gray,¹⁹ S. W. Gray,¹⁹ D. L. Hartill,¹⁹ B. K. Heltsley,¹⁹ D. Hertz,¹⁹ C. D. Jones,¹⁹ J. Kandaswamy,¹⁹ D. L. Kreinick,¹⁹ V. E. Kuznetsov,¹⁹ H. Mahlke-Krüger,¹⁹ T. O. Meyer,¹⁹ P. U. E. Onyisi,¹⁹ J. R. Patterson,¹⁹ D. Peterson,¹⁹ J. Pivarski,¹⁹ D. Riley,¹⁹ A. Ryd,¹⁹ A. J. Sadoff,¹⁹ H. Schwarthoff,¹⁹ X. Shi,¹⁹ S. Stroiney,¹⁹ W. M. Sun,¹⁹ T. Wilksen,¹⁹ M. Weinberger,¹⁹ S. B. Athar,²⁰ R. Patel,²⁰ V. Potlia,²⁰ J. Yelton,²⁰ P. Rubin,²¹ C. Cawfield,²² B. I. Eisenstein,²² I. Karliner,²² D. Kim,²² N. Lowrey,²² P. Naik,²² C. Sedlack,²² M. Selen,²² E. J. White,²² J. Wiss,²² and M. R. Shepherd²³

(CLEO Collaboration)

¹University of Kansas, Lawrence, Kansas 66045, USA

²Luther College, Decorah, Iowa 52101, USA

³University of Minnesota, Minneapolis, Minnesota 55455, USA

⁴Northwestern University, Evanston, Illinois 60208, USA

⁵State University of New York at Albany, Albany, New York 12222, USA

⁶University of Oklahoma, Norman, Oklahoma 73019, USA

⁷University of Pittsburgh, Pittsburgh, Pennsylvania 15260, USA

⁸University of Puerto Rico, Mayaguez, Puerto Rico 00681

⁹Purdue University, West Lafayette, Indiana 47907, USA

¹⁰Rensselaer Polytechnic Institute, Troy, New York 12180, USA

¹¹University of Rochester, Rochester, New York 14627, USA

¹²Southern Methodist University, Dallas, Texas 75275, USA

¹³Syracuse University, Syracuse, New York 13244, USA

¹⁴Vanderbilt University, Nashville, Tennessee 37235, USA

¹⁵Wayne State University, Detroit, Michigan 48202, USA

¹⁶Carleton University, Ottawa, Ontario, Canada K1S 5B6

¹⁷Carnegie Mellon University, Pittsburgh, Pennsylvania 15213, USA

¹⁸Enrico Fermi Institute, University of Chicago, Chicago, Illinois 60637, USA

¹⁹Cornell University, Ithaca, New York 14853

²⁰University of Florida, Gainesville, Florida 32611, USA

²¹George Mason University, Fairfax, Virginia 22030, USA

²²University of Illinois, Urbana-Champaign, Illinois 61801, USA

²³Indiana University, Bloomington, Indiana 47405, USA

(Received 12 July 2006; published 29 January 2007)

Using data collected with the CLEO III detector at the CESR e^+e^- collider, we report on a first observation of the decay $Y(3S) \rightarrow \tau^+ \tau^-$, and precisely measure the ratio of branching fractions of $Y(nS)$, $n = 1, 2, 3$, to $\tau^+ \tau^-$ and $\mu^+ \mu^-$ final states, finding agreement with expectations from lepton universality. We derive absolute branching fractions for these decays, and also set a limit on the influence of a low mass CP -odd Higgs boson in the decay of the $Y(1S)$.

DOI: 10.1103/PhysRevLett.98.052002

PACS numbers: 13.25.Gv, 14.40.Gx, 14.80.Cp

In the standard model, the couplings between leptons and gauge bosons are independent of the lepton flavor, so the branching fractions for the decay $Y(nS) \rightarrow l^+ l^-$

should be independent of the flavor of the lepton l , except for negligible lepton mass effects. Any deviation from unity for the ratio of branching fractions

$\mathcal{R}_{\tau\tau}^Y = B(Y(nS) \rightarrow \tau^+\tau^-)/B(Y(nS) \rightarrow \mu^+\mu^-)$ would indicate the presence of new physics. The ratio $\mathcal{R}_{\tau\tau}^Y$ is sensitive to the mechanism proposed in [1], in which a low mass CP -odd Higgs boson, A^0 , mediates the decay chain $Y(1S) \rightarrow \eta_b\gamma$, $\eta_b \rightarrow A^0 \rightarrow \tau^+\tau^-$.

CLEO has recently measured the partial width, Γ_{ee} , from $e^+e^- \rightarrow Y(nS)$ [2], $n = 1, 2, 3$, as well as the branching fraction for $Y(nS) \rightarrow \mu^+\mu^-$ [3]. This analysis complements these measurements by measuring $\mathcal{R}_{\tau\tau}^Y$ directly, and scales this result to obtain $B(Y(nS) \rightarrow \tau^+\tau^-)$. An upper limit on the product branching fraction $B(Y(1S) \rightarrow \eta_b\gamma)B(\eta_b \rightarrow A^0 \rightarrow \tau^+\tau^-)$ is extracted.

The data in this analysis were obtained with the CLEO III detector [4,5] at the symmetric e^+e^- collider CESR. The detector includes a precision tracking system in a solenoidal magnetic field, a CsI calorimeter, a Ring Imaging Cherenkov detector, and muon chambers. The data are identical to those in [3], including both on-resonance and off-resonance subsamples at the $Y(nS)$, $n = 1, 2, 3$. In addition, 0.5 fb^{-1} at the $Y(4S)$ and 0.6 fb^{-1} 40 MeV below the $Y(4S)$ peak were used as control samples.

The analysis technique, similar to that in [3], isolates the $Y \rightarrow \mu^+\mu^-$, $\tau^+\tau^-$ signals by subtracting a scaled number of events observed off resonance from the number observed in on-resonance data, and, after further background correction, attributes the remaining signal to $Y \rightarrow l^+l^-$. Selection criteria are developed to isolate $\mu^+\mu^-$ and $\tau^+\tau^-$ final states using a subset of the data acquired near the $Y(4S)$. Being dominated by strong interaction decays, the full width of the $Y(4S)$ is sufficiently large that $Y(4S) \rightarrow \tau^+\tau^-$ decays in our sample are negligible. Another subset of $Y(4S)$ data is used to verify that the scaled subtraction produces no signal for $Y(4S) \rightarrow \tau^+\tau^-$, $\mu^+\mu^-$, indicating that non- Y backgrounds are suppressed by the subtraction. Furthermore, the off-resonance production cross sections for $\tau^+\tau^-$ and $\mu^+\mu^-$ are verified to agree with theoretical expectations.

The final states chosen for both the $Y \rightarrow \mu^+\mu^-$ and $Y \rightarrow \tau^+\tau^-$ decays are required to have exactly two good quality charged tracks of opposite charge. In this Letter, \sqrt{s} denotes the total available center of mass energy, X_p is a particle's momentum, P , scaled to the beam energy, E_{beam} . The energy deposited by a particle in the calorimeter is E_{CC} .

Selection criteria for the $\mu^+\mu^-$ final state closely follow those of [3], requiring tracks with $0.7 < X_p < 1.15$, of which at least one is positively identified as a muon, using both the muon chambers and the calorimeter. The opening angle between the associated momenta must be greater than 170° . Events must have no more than one isolated shower that is unassociated with a track and has energy greater than 1% of the beam energy.

At least two neutrinos from final states of $e^+e^- \rightarrow \tau^+\tau^-$ escape detection. Due to CLEO III's almost hermetic

acceptance, the following criteria select such events despite the energy carried away by the unreconstructed neutrinos. The total charged-track momentum transverse to the beam direction must be greater than 10% of E_{beam} , and the total charged-track momentum must point into the barrel region of the detector where tracking and calorimetry are optimal. Events with collinear tracks are eliminated. Tracks are required to have $0.1 < X_p < 0.9$, where the upper limit is chosen to minimize pollution from two-particle final states. The total observed energy due to charged and neutral particles in the calorimeter is similarly required to be between $0.2\sqrt{s}$ and $0.9\sqrt{s}$. To reduce overlap confusion between neutral and charged particles, tracks and associated showers must satisfy $E_{CC}/P < 1.1$. Potential backgrounds due to cosmic rays are accounted for as in [3]. In all cases these were negligible.

Final states are further exclusively divided according to the results of particle identification into (e, e) , (μ, e) , (e, μ) , (μ, μ) , (e, X) , (μ, X) , (X, X) subsamples, with particles listed in descending momentum order. The first (second) particle listed is referred to as the tag (signal). Lepton identification requires $P > 500 \text{ MeV}$ to ensure that the track intersects the calorimeter. Electrons are identified by requiring that $0.85 < E_{CC}/P < 1.10$, and that the specific ionization along the track's path in the drift chamber be consistent with the expectation for an electron. A muon candidate in τ decays is a charged track which is not identified as an electron, having $P > 2 \text{ GeV}/c$ ($> 1.5 \text{ GeV}/c$) for a tag (signal) track and confined to the central barrel where beam related background is a minimum. Furthermore, the muon candidate must penetrate at least three interaction lengths into the muon detector, and satisfy $100 \text{ MeV} < E_{CC} < 600 \text{ MeV}$. The missing momentum and energy criteria ensure that virtually all pions mistakenly identified as muons come from τ pair decays and are properly accounted for in the simulation, as shown by the agreement of off-resonance cross sections with expectations. Particles identified as neither e nor μ are designated X , and are a mixture of hadrons and unidentified leptons.

The decay products of τ pairs from Y decays tend to be separated into distinct hemispheres. Since the photon spectrum expected in τ decays depends on the identity of the charged particle, calorimeter showers are assigned to either the tag or signal hemisphere according to their proximity to the tag-side track direction. This separation into distinct hemispheres is not perfect, so there is some correlation between the photon spectrum on tag and signal sides of the event. The modes with two identified leptons each require fewer than 6 showers and a maximum shower energy below $0.1E_{\text{beam}}$. Defining $E_{\text{neut}}^{\text{tag}}$ ($E_{\text{neut}}^{\text{sig}}$) as the total isolated shower energy in the calorimeter on the tag (signal) sides of the event, the (e, e) mode assignment requires $E_{\text{neut}}^{\text{tag}} < 0.1E_{\text{beam}}$ and $E_{\text{neut}}^{\text{sig}} < 0.1E_{\text{beam}}$, while the (μ, e) , (e, μ) , and (μ, μ) modes require $E_{\text{neut}}^{\text{tag}} < 0.2E_{\text{beam}}$

and $E_{\text{neut}}^{\text{sig}} < 0.2E_{\text{beam}}$. The (e, X) , (μ, X) , and (X, X) modes all require that $E_{\text{neut}}^{\text{tag}} < 0.4E_{\text{beam}}$ and $E_{\text{neut}}^{\text{sig}} < 0.4E_{\text{beam}}$. In addition, the (e, X) mode requires fewer than 4 unassociated showers with energies above $0.4E_{\text{beam}}$.

For the (e, e) and (μ, μ) modes, contamination from radiative dileptons is reduced by requiring $P_{\text{tag}} + P_{\text{sig}} < 1.5E_{\text{beam}}$. To reduce backgrounds from $e^+e^- \rightarrow l^+l^-\gamma\gamma$ and $e^+e^- \rightarrow e^+e^-l^+l^-$ in the (e, e) , (μ, μ) , (X, X) categories, the minimum polar angle of any unseen particles, deduced from energy-momentum conservation, is required to point into the barrel region, where calorimetry cuts will ensure rejection.

Figure 1 shows the superimposed on-resonance and scaled off-resonance total energy distributions for the $\tau^+\tau^-$ sample for all resonances. The scale factor is $\mathcal{S} = (\mathcal{L}_{\text{on}}/\mathcal{L}_{\text{off}})(s_{\text{off}}/s_{\text{on}})\delta_{\text{interf}}$, where \mathcal{L} and s are the data luminosity and squared center of mass collision energies on and off the resonances, and δ_{interf} is an interference correction. The luminosity is derived from the process $e^+e^- \rightarrow \gamma\gamma$ [6], which does not suffer backgrounds from direct Y decays. The interference correction δ_{interf} accounts for the small interference between the process $e^+e^- \rightarrow ll$ and $e^+e^- \rightarrow Y \rightarrow ll$ and is estimated [3] to be 0.984 (0.961, 0.982) at the $Y(1S)$ ($2S$, $3S$) and negligible for the $Y(4S)$. The interference largely cancels in the ratios considered in this Letter. The agreement of the distributions for the $Y(4S)$, which also extends to individual subsamples, validates the subtraction technique, and highlights the absence of any process whose cross section does not vary as $1/s$. This agreement also indicates that no Monte Carlo simulation is needed to subtract continuum production from $Y(nS)$ data.

The ratio of measured relative lepton pair production cross-sections at the off-resonance points, $\mathcal{R}_{\tau\tau}^{\text{off}} =$

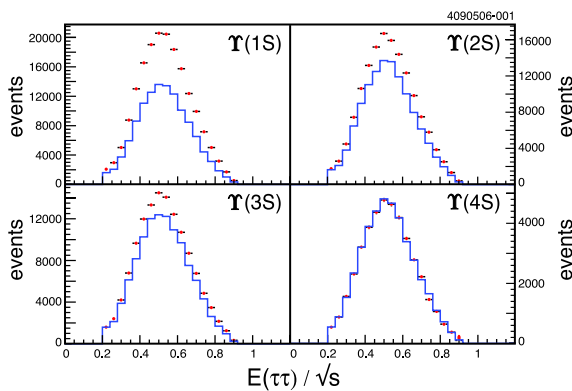


FIG. 1 (color online). Total energy distributions, scaled to center of mass energy, $E_{\tau\tau}/\sqrt{s}$ for the $\tau^+\tau^-$ final states at the $Y(nS)$, $n = 1, 2, 3, 4$ on (points) and scaled off (histograms) resonance. The excess of on-resonance relative to scaled off-resonance data is attributed to $Y(nS)$, $n = 1, 2, 3$ decays. The agreement at the $Y(4S)$ tests the validity of the subtraction technique.

$\sigma_{\tau\tau}/\sigma_{\mu\mu}$, with respect to that theoretically expected, $\mathcal{R}_{\tau\tau}^{\text{off th}}$, is $\mathcal{R}_{\tau\tau}^{\text{off}}/\mathcal{R}_{\tau\tau}^{\text{off th}} = 0.96 \pm 0.03$ (0.97 ± 0.03 , 0.97 ± 0.03 , 1.00 ± 0.03) below the $Y(1S)$ ($2S$, $3S$, $4S$) for the sum of all τ decay mode pairs, with statistical and systematic uncertainties added in quadrature. The expectation $\mathcal{R}_{\tau\tau}^{\text{off th}} = 0.83 \pm 0.02(\text{syst})$ [7] is found to be numerically independent of the particular resonance considered. The reconstruction efficiencies are derived from the FPAIR [8] and KORALB-TAUOLA [9–11] Monte Carlo simulations. Backgrounds were corrected by using $e^+e^- \rightarrow q\bar{q}$ ($q = u, d, c, s$) simulations [11–14]. The scatter in the central values of $\mathcal{R}_{\tau\tau}^{\text{off}}/\mathcal{R}_{\tau\tau}^{\text{off th}}$ indicates that systematic uncertainties are small.

The reconstruction efficiency for observing $Y \rightarrow \mu^+\mu^-$ is derived from the CLEO GEANT-based simulation [11–14], as shown in Table I. This efficiency is found to be constant across the resonances. The reconstruction efficiency for observing $Y \rightarrow \tau^+\tau^-$ is derived using the KORALB-TAUOLA event generator integrated into the detector simulation. Although this generator models the process $e^+e^- \rightarrow \gamma^* \rightarrow \tau^+\tau^-$, the quantum numbers of the Y and γ are the same so it can be used as long as initial state radiation (ISR) effects are not included. This efficiency is found to be consistent across all resonances within any given $\tau^+\tau^-$ decay channel.

Results of the subtraction are summarized in Table I, showing the first observation of $Y(3S) \rightarrow \tau^+\tau^-$.

Backgrounds resulting from cascade decays within the $b\bar{b}$ system to ll are estimated using the Monte Carlo simulation, with branching fractions scaled to the values measured in this study. Cascade backgrounds with non- $\mu^+\mu^-$ and non- $\tau^+\tau^-$ final states are estimated directly from the Monte Carlo simulation.

Figure 2 displays the off-resonance subtracted data, superimposed on Monte Carlo expectations. The distributions shown are P_{tag} , P_{sig} , and $E_{\tau\tau}$ for a sampling of τ

TABLE I. Events yields for $Y \rightarrow \mu^+\mu^-$ (top) and $Y \rightarrow \tau^+\tau^-$ (bottom). Shown are the number of events (\tilde{N}_{ll}) after subtraction of backgrounds estimated from scaled off-resonance data and Y feedthrough estimated from the Monte Carlo simulation, the signal efficiency [$\epsilon(ll)$], and the total efficiency corrected number of signal events $N(Y \rightarrow ll) = \tilde{N}_{ll}/\epsilon(ll)$. The $\tau^+\tau^-$ events are summed over all τ decay modes. Uncertainties include data and Monte Carlo statistical uncertainties, uncertainties on backgrounds, and detector modeling [included only for $\epsilon(\mu^+\mu^-)$ to avoid double counting in the final ratio].

	Y(1S)	Y(2S)	Y(3S)
$\tilde{N}(\mu^+\mu^-)$ (10^3)	345 ± 7	121 ± 7	82 ± 7
$\epsilon(\mu^+\mu^-)$ (%)	65.4 ± 1.2	65.0 ± 1.1	65.1 ± 1.2
$N(Y \rightarrow \mu^+\mu^-)$ (10^3)	527 ± 15	185 ± 11	126 ± 11
$\tilde{N}(\tau^+\tau^-)$ (10^3)	60.1 ± 1.5	21.8 ± 1.5	14.8 ± 1.5
$\epsilon(\tau^+\tau^-)$ (%)	11.2 ± 0.1	11.3 ± 0.1	11.1 ± 0.1
$N(Y \rightarrow \tau^+\tau^-)$ (10^3)	537 ± 14	193 ± 12	132 ± 13

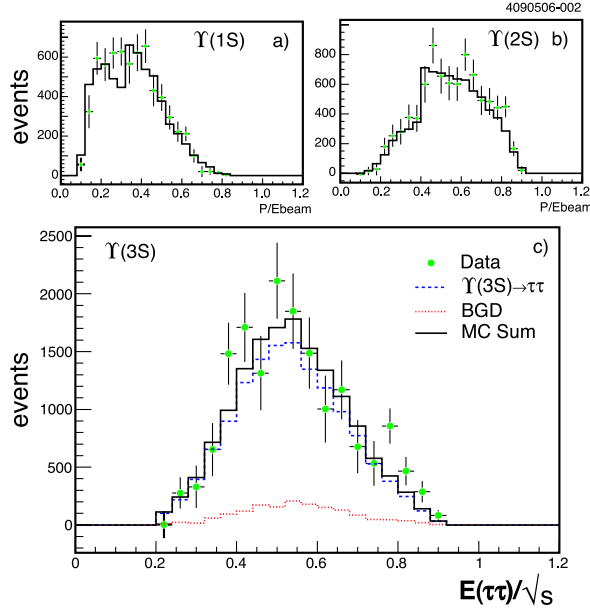


FIG. 2 (color online). Distributions for the $\tau^+\tau^-$ final states at the $Y(nS)$, $n = 1, 2, 3$ after subtraction of \mathcal{S} -scaled off-resonance data. The solid line shows the expected total signal and background distributions, assuming lepton universality. (a) $P_{\text{sig}}/E_{\text{beam}}$ in $Y(1S)$ decays for the sum of τ decay modes including exactly two identified leptons, (b) $P_{\text{tag}}/E_{\text{beam}}$ in $Y(2S)$ decays for τ modes including exactly one identified lepton, (c) $E_{\tau\tau}/\sqrt{s}$ for $Y(3S)$ for the sum of all τ modes, where signal and total background distributions are explicitly displayed. Uncertainties are statistical. The steps observed in (a), (b) are due to momentum criteria in muon identification.

decay modes. In all cases the Monte Carlo expectation is consistent with the data assuming lepton universality and branching fractions from [3]. The agreement across the various kinematic quantities indicates that backgrounds are well controlled.

Figure 3 shows the agreement across all $\tau^+\tau^-$ subsamples of the ratio of off-resonance cross sections for $\tau^+\tau^-$ and $\mu^+\mu^-$ production, relative to expectation, as well as the ratio of branching fractions for each of these decay modes at the different Y resonances, relative to the expectation $\mathcal{R}_{\tau\tau}^{Y\text{th}} = 1$. The agreement across $\tau^+\tau^-$ subsamples both on and off the resonances is again an indication that backgrounds are small and well estimated.

The ratio of branching fractions and final branching fractions are listed in Table II. These results show that lepton universality is respected in Y decay within the $\approx 10\%$ measurement uncertainties.

Systematic uncertainties, summarized in Table III, are estimated for the ratio of branching fractions, and for the absolute branching fraction. The ratio is insensitive to some common systematic uncertainties.

Most systematic uncertainties due specifically to ll selection are derived by a variation of the selection criteria over reasonable ranges in the $Y(1S)$ sample, which has the

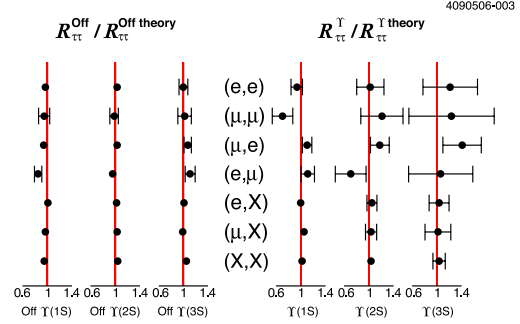


FIG. 3 (color online). Breakdown by mode of off- and on-resonance data at the different resonances. On the left, the ratio of the production cross section for $e^+e^- \rightarrow ll$ ($l = \tau, \mu$), relative to its expectation, is plotted for data taken below the Y for each τ decay mode pair. On the right, the ratio of branching fractions for the process $Y(nS) \rightarrow ll$ ($l = \tau, \mu$, $n = 1, 2, 3$) relative to the expectation $\mathcal{R}_{\tau\tau}^{Y\text{th}} = 1$ is displayed. The lines represent the standard model expectation. Errors shown are statistical.

lowest energy released in its decay. The most significant of these are due to momentum selection (1.3%), calorimeter energy selection (1.1%), and angular selection (1.1%). The systematic uncertainty due to modeling of the trigger is estimated to be 1.6%.

Backgrounds are assumed to be from Y decays, chiefly due to cascade decays to lower resonances, and are estimated to be 2.5% (15%, 11%) of the $\tau^+\tau^-$ sample at the $Y(1S)(2S, 3S)$, with an estimated uncertainty contribution to $\mathcal{R}_{\tau\tau}^Y$ of 0.1% (2.4%, 1.3%).

The uncertainty due to detector modeling in [3] was estimated to be 1.7%: this value is used here conservatively for the systematic uncertainty on the ratio.

The modeling of the physics in $Y(1S) \rightarrow \mu^+\mu^-$, obtained by varying the decay model for $Y \rightarrow \mu^+\mu^-$ between the Monte Carlo simulation and KORALB with ISR simulation turned off, contributes a 2% uncertainty. This is consistent with the variation in the product $\epsilon(\mu^+\mu^-)\sigma_{ee \rightarrow \mu\mu}$ using the FPAIR, KORALB, and BABAYAGA [15] Monte Carlo simulations, and is thus likely conservative, as direct $\mu^+\mu^-$ production from the Y at the peak involves much lower energy final state photons than off-resonance production. An uncorrelated uncertainty of 2% for modeling of $Y \rightarrow \tau^+\tau^-$ is assumed, consistent with

TABLE II. Final results on the ratio of branching fractions to $\tau^+\tau^-$ and $\mu^+\mu^-$ final states, and the absolute branching fraction for $Y \rightarrow \tau^+\tau^-$. Included are both statistical and systematic uncertainties, as detailed in the text. Results from Ref. [3] are used in deriving the final absolute branching fractions.

	$\mathcal{R}_{\tau\tau}^Y$	$B(Y \rightarrow \tau^+\tau^-)$ (%)
$Y(1S)$	$1.02 \pm 0.02 \pm 0.05$	$2.54 \pm 0.04 \pm 0.12$
$Y(2S)$	$1.04 \pm 0.04 \pm 0.05$	$2.11 \pm 0.07 \pm 0.13$
$Y(3S)$	$1.05 \pm 0.08 \pm 0.05$	$2.52 \pm 0.19 \pm 0.15$

TABLE III. Summary of systematic uncertainties for the $Y(nS)$, $n = 1/2/3$. The entry $\sigma(\mathcal{R}_{\tau\tau}^Y)/\mathcal{R}_{\tau\tau}^Y$ is the relative uncertainty on $\mathcal{R}_{\tau\tau}^Y$, while $\sigma(B_{\tau\tau})/B_{\tau\tau}$ indicates uncertainties specific to τ decay modes used in addition to those in [3] to obtain $B(Y \rightarrow \tau^+\tau^-)$. The uncertainty on \mathcal{S} and the background are included in the statistical uncertainty as they depend chiefly on measurements made in this Letter.

Source	σ_{syst} (%)
\mathcal{S}	0.2/0.4/0.3
Background	0.1/2.4/1.3
τ , μ selection	2.9/2.9/2.9
$Y \rightarrow \mu^+\mu^-$ model	2.0/2.0/2.0
$Y \rightarrow \tau^+\tau^-$ model	2.0/2.0/2.0
Detector model	1.7/1.7/1.7
MC statistics	1.9/1.0/1.0
$\sigma(\mathcal{R}_{\tau\tau}^Y)/\mathcal{R}_{\tau\tau}^Y$	4.8/4.4/4.6
$\sigma(B_{\tau\tau})/B_{\tau\tau}$	4.0/3.8/3.9

previous analyses, and is again conservative as on-resonance production of $\tau^+\tau^-$ final states involves fewer photons than direct continuum production. To test the sensitivity to ISR simulation, the reconstruction efficiency for events with no ISR simulation is compared to that for events generated with ISR simulation turned on and re-weighted according to the relative value of the Y line shape at the τ pair mass. These efficiencies agree to within 0.8%.

The existence of a CP -odd Higgs boson, A^0 , with a mass near the $Y(1S)$, could induce a value of $\mathcal{R}_{\tau\tau}^Y$ not equal to one through its participation in the decay chain $Y(1S) \rightarrow \eta_b \gamma$, $\eta_b \rightarrow A^0 \rightarrow \tau^+\tau^-$, as detailed in [1]. By assuming that the mass of the $\eta_b(1S)$ is 100 MeV/ c^2 below the $Y(1S)$ mass, consistent with the largest value in [16], the value quoted for $\mathcal{R}_{\tau\tau}^Y(1S)$ can be translated into an upper limit on the combined branching fraction of $B(Y(1S) \rightarrow \eta_b \gamma)B(\eta_b \rightarrow A^0 \rightarrow \tau\tau) < 0.27\%$ at 95% confidence level, including systematic uncertainties. Since the transition photon is not explicitly reconstructed, this limit is valid for all η_b that approximately satisfy $(M[Y(1S)] - M[\eta_b] + \Gamma[\eta_b]) < \mathcal{O}(100 \text{ MeV}/c^2)$.

In summary, using the full sample of on-resonance $Y(nS)$, $n = 1, 2, 3$ CLEO III data, we have made the first observation of the decay $Y(3S) \rightarrow \tau^+\tau^-$ and precision measurement of its branching fraction. We have reported the ratio of branching fractions of Y decays to $\tau^+\tau^-$ and $\mu^+\mu^-$ final states, and find these to be consistent with expectations from the standard model. These ratios have been combined with results from [3] to provide absolute branching fractions for the process $Y \rightarrow \tau^+\tau^-$, resulting in the most precise single measurement of $B(Y(1S) \rightarrow \tau^+\tau^-)$ [17], and a much improved value of $B(Y(2S) \rightarrow \tau^+\tau^-)$. The ratio of branching fractions for $\tau^+\tau^-$ and $\mu^+\mu^-$ final states has also been used to set a limit on a possible Higgs mediated decay window.

We gratefully acknowledge the effort of the CESR staff in providing us with excellent luminosity and running conditions. We also thank M.A. Sanchis-Lozano for many illuminating discussions. This work was supported by the A.P. Sloan Foundation, the National Science Foundation, the US Department of Energy, and the Natural Sciences and Engineering Research Council of Canada.

*Current address: Universität Bonn; Nussallee 12; D-53115 Bonn, Germany.

- [1] M. A. Sanchis-Lozano, *Int. J. Mod. Phys. A* **19**, 2183 (2004).
- [2] J. L. Rosner *et al.* (CLEO Collaboration), *Phys. Rev. Lett.* **96**, 092003 (2006).
- [3] G. Adams *et al.* (CLEO Collaboration), *Phys. Rev. Lett.* **94**, 012001 (2005).
- [4] G. Viehhauser, *Nucl. Instrum. Methods Phys. Res., Sect. A* **462**, 146 (2001); D. Peterson *et al.*, *Nucl. Instrum. Methods Phys. Res., Sect. A* **478**, 142 (2002); M. Artuso *et al.*, *Nucl. Instrum. Methods Phys. Res., Sect. A* **554**, 147 (2005).
- [5] Y. Kubota *et al.* (CLEO Collaboration), *Nucl. Instrum. Methods Phys. Res., Sect. A* **320**, 66 (1992); D. Bortoletto *et al.*, *Nucl. Instrum. Methods Phys. Res., Sect. A* **320**, 114 (1992).
- [6] G. Crawford *et al.* (CLEO Collaboration), *Nucl. Instrum. Methods Phys. Res., Sect. A* **345**, 429 (1994).
- [7] This expectation is lower than 1 because of the larger phase space available for initial state radiation production of $\mu^+\mu^-$ relative to $\tau^+\tau^-$ final states.
- [8] R. Kleiss and S. van der Marck, *Nucl. Phys.* **B342**, 61 (1990).
- [9] S. Jadach and Z. Wąs, *Acta Phys. Pol. B* **15**, 1151 (1984); **16**, 483(E) (1985); S. Jadach and Z. Wąs, *Comput. Phys. Commun.* **36**, 191 (1985); **64**, 267 (1991); **85**, 453 (1995).
- [10] S. Jadach, J. H. Kühn, and Z. Wąs, *Comput. Phys. Commun.* **64**, 275 (1991); M. Jezabek, Z. Wąs, S. Jadach, and J. H. Kühn, *ibid.* **70**, 69 (1992); S. Jadach and Z. Wąs, *ibid.* **76**, 361 (1993); R. Decker, E. Mirkes, R. Sauer, and Z. Wąs, *Z. Phys. C* **58**, 445 (1993).
- [11] E. Barberio, B. van Eijk, and Z. Wąs, *Comput. Phys. Commun.* **66**, 115 (1991); E. Barberio and Z. Wąs, *Comput. Phys. Commun.* **79**, 291 (1994).
- [12] R. Brun *et al.*, GEANT 3.21, CERN Program Library Long Writeup Report No. W5013, 1993.
- [13] T. Sjöstrand *et al.*, *Comput. Phys. Commun.* **135**, 238 (2001).
- [14] QQ-The CLEO Event Generator, <http://www.lns.cornell.edu/public/CLEO/soft/qq>.
- [15] C. M. Carloni Calame *et al.*, *Nucl. Phys. B, Proc. Suppl.* **131**, 48 (2004).
- [16] S. Godfrey and J. L. Rosner, *Phys. Rev. D* **64**, 074011 (2001); **65**, 039901(E) (2002).
- [17] W.-M. Yao *et al.* (Particle Data Group), *J. Phys. G* **33**, 1 (2006).